Variational Analysis of Ridged Waveguide Modes

YOZO UTSUMI, MEMBER, IEEE

Abstract—**Brief expressions of eigenvalue problems, normal modes, and electric-field profiles for all odd TE and TM modes of ridged waveguides, and the guide wavelength and characteristic impedance for the TE_{10} dominant mode, are presented in this paper.**

In this analysis, the computation time can be reduced by getting simple approximated variational expressions for eigenvalue equations by using a trial function which satisfies the right-angled edge condition of a ridge.

These theoretical results are in good agreement with the experimental results and the several references employed.

I. Introduction

APPLICATIONS of ridged waveguides have been of wide-ranging use in microwave devices and circuits, and research on them has been continued steadily. In 1947, Cohn [1] obtained ridged waveguide eigenvalues of TE_{mo} modes by using the transverse resonance method in a cross section of a ridged waveguide. Hopfer [2] and Pyle [3] published further improved approximated analyses for eigenvalue problems of TE_{mo} modes. In 1962, Getsinger [4] first published approximated field equations of the TE_{10} mode. Getsinger assumed the TEM mode under the gap and made the matching condition only in electric fields. In 1971, Montgomery [5] published the complete solutions of ridged waveguide eigenvalue problems for all TE and TM modes. In this method, an eigenvalue equation was given in a matrix form, and an integral eigenvalue equation was subsequently solved numerically by application of the Ritz–Galerkin method. In a recent paper, an approximated closed-form expression for the eigenvalue problem of the TE_{10} mode was published for concentrating on the reduction of computation time [6]. And also for the eigenvalue problem of the finline, Schmidt and Itoh published the spectrum-domain analysis [7], where the field at the top of the fin was assumed as the near field of the 0° angle conductor edge.

On the other hand, a planar circuit mounted in a waveguide (PCMW) was proposed by Konishi [8] as an effective application of a ridged waveguide, and a 12-GHz band low-noise down converter with a PCMW was developed [9], [10] for satellite broadcasting by the NHK Technical Research Laboratories. In the theoretical design of this down converter, it becomes important to determine the equivalent circuits of several discontinuities in a ridged waveguide. Therefore, a theoretical analysis with short computation time for eigenvalue problems and normal mode expressions including all TE and TM modes of a ridged waveguide becomes important. It is impossible to meet this requirement by using theoretical methods found in [1]–[4] and [6]. Although Montgomery's method [5] is powerful and can meet this requirement in the main, it cannot be regarded as an economical method in view of computation time.

In this present paper, the near field of the edge of a ridge is expressed by a known distribution function as described in [7] in the case of a finline. In the case of a ridged waveguide, as the thickness of the ridge is finite, the ridge edge has a right angle different from the 0° angle of the finline's infinitely thin edge. And it becomes complicated to use the spectrum-domain analysis of [7], because two different spectrum domains exist on both sides of the edge. In this paper, in selecting a trial function which satisfies the edge condition of a ridge, the variational method [11] is used in real space (x, y plane). By using the simple approximated eigenvalue equation, this analysis has met the requirement, described above, of short computation time. This paper also gives the normal mode expression and the electric-field profile of each mode, the guide wavelength, and the characteristic impedance for the dominant mode. Finally, by comparing these theoretical results with experimental ones and others [2], [4], [5], the correctness of this analysis is confirmed.

II. Wave Equations and Boundary Conditions

The cross-sectional shape of the ridged waveguide with the coordinates is illustrated in Fig. 1, where $2t$ means the thickness of the ridge, s the gap in the ridge, $2a \times b$ waveguide dimensions, I the region of $0 \leqslant x \leqslant t$, and II the region of $t \leqslant x \leqslant a$. All ridged waveguide modes can be classified into TE or TM modes, and these fields are derivable from two kinds of scalar potentials ψ_{pi}, and $\psi_{pi}(x, y, z) = \phi_{pi}(x, y) \cdot g_{pi}(z)$. ϕ_{pi} is a function of only the transverse coordinate. This potential function ϕ_{pi} satisfies a wave equation

$$\nabla_t^2 \phi_{pi} + k_T^2 \phi_{pi} = 0 \tag{1}$$

where

$$p = \begin{cases} h : \phi_{hi} \text{ indicates magnetic scalar potential} \\ e : \phi_{ei} \text{ indicates electric scalar potential} \end{cases}$$

$$i = \begin{cases} 1 : \phi_{p1} \text{ indicates scalar potential for region I} \\ 2 : \phi_{p2} \text{ indicates scalar potential for region II} \end{cases}$$

$k_T^2 = k_0^2 - \beta^2$.

Manuscript received March 29, 1984; revised July 13, 1984.

The author is with Technical Research Laboratories of NHK, 1-10-11 Kinuta, Setagaya, Post No. 157, Tokyo, Japan.

0018-9480/85/0002-0111$01.00 ©1985 IEEE

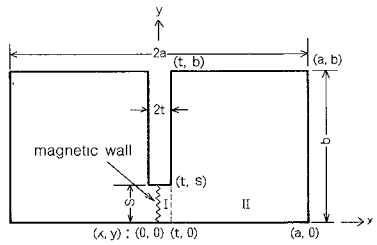

Fig. 1. Cross-sectional shape of a ridged waveguide with coordinates.

In (1), $\nabla_t^2 = \partial^2/\partial x^2 + \partial^2/\partial y^2$, k_T is a ridged waveguide eigenvalue, β is a propagation constant in the z direction, and k_0 the propagation constant in free space.

Two scalar potential functions are related to the electric and magnetic fields of TE and TM modes by [12]:

for TE modes

$$\begin{aligned} \boldsymbol{E}_{ti} &= \boldsymbol{i}_z \times \nabla_t \phi_{hi}(x, y) \\ \boldsymbol{H}_{ti} &= -\beta/(\omega\mu_0)\cdot\nabla_t \phi_{hi}(x, y) \\ \boldsymbol{H}_{zi} &= j\boldsymbol{i}_z\left(\beta^2 - k_0^2\right)/(\omega\mu_0)\cdot\phi_{hi}(x, y) \end{aligned} \tag{2a}$$

for TM modes

$$\begin{aligned} \boldsymbol{E}_{ti} &= -\beta/(\omega\varepsilon_0)\cdot\nabla_t \phi_{ei}(x, y) \\ \boldsymbol{E}_{zi} &= j\boldsymbol{i}_z\left(\beta^2 - k_0^2\right)/(\omega\varepsilon_0)\cdot\phi_{ei}(x, y) \\ \boldsymbol{H}_{ti} &= \nabla_t \phi_{ei}(x, y)\times\boldsymbol{i}_z \end{aligned} \tag{2b}$$

where $g_{pi}(z)$ is omitted, and $\boldsymbol{i}_z$ is a unit vector of the z direction, $j = \sqrt{-1}$, ε_0 and μ_0 are the permittivity and permeability of free space, respectively, ω is the angular frequency, the suffix t means the transverse direction (x, y), and $\nabla_t = \boldsymbol{i}_x(\partial/\partial_x) + \boldsymbol{i}_y(\partial/\partial_y)$.

Considering the odd TE and TM modes whose symmetry plane has been assumed as the y coordinate axis $(x = 0)$ in this analysis, the $x = 0$ plane can be regarded as a magnetic wall. In the case of the even modes, a similar analysis can be accomplished, regarding the $x = 0$ plane as an electric wall. Therefore, in the following discussion, the $x = 0$ plane is regarded as a magnetic wall and only a half of the ridged waveguide $(0 \leqslant x \leqslant a)$ is considered.

In Fig. 1, it is necessary to satisfy the boundary conditions on the conductor surface and the magnetic wall for both TE and TM modes:

for TE modes

$$\begin{aligned} \frac{\partial \phi_{hi}}{\partial n} &= 0, && \text{on conductor surface} \\ \phi_{hi} &= 0, && \text{on magnetic wall} \end{aligned} \tag{3a}$$

for TM modes

$$\begin{aligned} \phi_{ei} &= 0, && \text{on conductor surface} \\ \frac{\partial \phi_{ei}}{\partial n} &= 0, && \text{on magnetic wall} \end{aligned} \tag{3b}$$

where $\boldsymbol{n} = \boldsymbol{i}_n n$, the normal vector on each surface or wall as shown in Fig. 2.

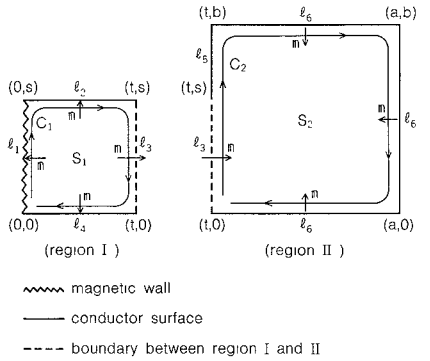

Fig. 2. Contour pass C_i for integral representations in (6).

III. Variational Principle for Eigenvalue Problems

A. Stationary Formula

We have the following variational expressions for TE modes:

$$k_T^2 = -\frac{\sum_{i=1}^{2}\langle\phi_{hi}\cdot\nabla_t^2\phi_{hi}\rangle_{S_i} + \sum_{i=1}^{2}\langle\phi_{hi}\cdot\frac{\partial\phi_{hi}}{\partial n}\rangle_{C_i}}{\sum_{i=1}^{2}\langle\phi_{hi}^2\rangle_{S_i}} \tag{4a}$$

where the constraint conditions for the trial eigenfunction ϕ_{hi} are given by

$$\begin{aligned} \frac{\partial \phi_{hi}}{\partial n} &= 0, && \text{on } l_2,\ l_4,\ l_5, \text{ and } l_6 \\ \frac{\partial \phi_{h1}}{\partial n} &= \frac{\partial \phi_{h2}}{\partial n} = \xi(y), && \text{on } l_3 \end{aligned} \tag{4b}$$

$$\begin{aligned} \xi(y) &= 0, && \text{on } l_5 \\ \eta(y) &= 0, && \text{on } l_3 \text{ and } l_5 \end{aligned} \tag{4c}$$

where the trial distribution function $\xi(y)$ and $\eta(y)$ are proportional to the y and z components of the electric fields on l_3 and l_5, respectively.

For TM modes

$$k_T^2 = -\frac{\sum_{i=1}^{2}\langle\phi_{ei}\cdot\nabla_t^2\phi_{ei}\rangle_{S_i} - \sum_{i=1}^{2}\langle\phi_{ei}\cdot\frac{\partial\phi_{ei}}{\partial n}\rangle_{C_i}}{\sum_{i=1}^{2}\langle\phi_{ei}^2\rangle_{S_i}} \tag{5a}$$

where the constraint conditions for the trial eigenfunction ϕ_{ei} are given by

$$\phi_{ei} = 0, \qquad \text{on } l_2,\ l_4,\ l_5, \text{ and } l_6 \tag{5b}$$

$$\phi_{e1} = \phi_{e2} = \eta(y), \qquad \text{on } l_3 \tag{5c}$$

$$\eta(y) = 0, \qquad \text{on } l_5.$$

The relation between $\eta(y)$ and $\xi(y)$ is described later for the TM modes. The integral $\langle A\rangle_{S_i}$ for the cross-sectional area S_i and the contour integral $\langle A\rangle_{C_i}$ for the contour pass

C_i are defined as

$$\langle A\rangle_{S_1}=\int_0^s\int_0^t A\cdot dx\cdot dy$$

$$\langle A\rangle_{S_2}=\int_0^b\int_t^a A\cdot dx\cdot dy$$

$$\langle A\rangle_{C_1}=\int_0^s A|_{x=0}\cdot dy+\int_0^t A|_{y=s}\cdot dx+\int_s^0 A|_{x=t}\cdot dy+\int_t^0 A|_{y=0}\cdot dx$$

$$=\int_{l_1}A\cdot dl+\int_{l_2}A\cdot dl+\int_{l_3}A\cdot dl+\int_{l_4}A\cdot dl$$

$$\langle A\rangle_{C_2}=\int_0^s A|_{x=t}\cdot dy+\int_s^b A|_{x=t}\cdot dy+\int_t^a A|_{y=b}\cdot dx+\int_b^0 A|_{x=a}\cdot dy+\int_a^t A|_{y=0}\cdot dx$$

$$=-\int_{l_3}A\cdot dl-\int_{l_5}A\cdot dl-\int_{l_6}A\cdot dl. \tag{6}$$

In Appendix I, we have proved that if ϕ_{hi} and ϕ_{ei} minimize (4a) and (5a) with the constraint conditions (4b) and (4c), or (5b) and (5c), respectively, then they are the correct solutions of (1) with proper boundary conditions.

B. Trial Eigenfunction Including Eigenvalues

Equation (4a) can be transformed into

$$\sum_{i=1}^{2}\langle\phi_{hi}\cdot\nabla_t^2\phi_{hi}\rangle_{S_i}+k_T^2\cdot\sum_{i=1}^{2}\langle\phi_{hi}^2\rangle_{S_i}+\sum_{i=1}^{2}\langle\phi_{hi}\cdot\frac{\partial\phi_{hi}}{\partial n}\rangle_{C_i}=0 \tag{7a}$$

$$F=\text{left-hand side of (7a)}. \tag{7b}$$

It can be proven easily that F given by (7b) is also stationary for ϕ_{hi} from the stationary formula of (4a).

Next, we consider the cases of using the trial eigenfunction which includes the eigenvalue k_T in order to obtain the simplified stationary formula for the eigenvalue problem. When the trial eigenfunction is a function of the eigenvalue k_T, the closed-form expression of k_T cannot be obtained from (7a). In such a case, k_T is still stationary. We will prove it as follows.

When the trial eigenfunction is a function of the eigenvalue k_T and a parameter p_2 described as $\phi_{hi}(k_T, p_2)$, taking the first variations of k_T^2 and p_2 in (7a), and using the stationary character of (7b), the following relation is derived in Appendix II as

$$\delta k_T^2=0 \tag{8}$$

where a parameter p_2 is described in Appendix II.

Since the first variation of k_T^2 vanishes, the value of k_T^2 derived from (7a) is stationary. A similar expression for TM modes can be derived from (5a) as

$$\sum_{i=1}^{2}\langle\phi_{ei}\cdot\nabla_t^2\phi_{ei}\rangle_{S_i}+k_T^2\cdot\sum_{i=1}^{2}\langle\phi_{ei}^2\rangle_{S_i}-\sum_{i=1}^{2}\langle\phi_{ei}\cdot\frac{\partial\phi_{ei}}{\partial n}\rangle_{C_i}=0. \tag{9}$$

The left-hand side of (9) is also stationary for ϕ_{ei}.

IV. Stationary Formula for Ridged Waveguide

Applying the TE constraint conditions on l_2 and l_4 that $\partial\phi_{h1}/\partial n=0$ and the TE boundary condition on l_1 that $\phi_{h1}=0$, we find the trial eigenfunction in region I ($0\leqslant x\leqslant t$) to be

$$\phi_{h1}=\sum_{m=0}^{\infty}a_{hm}\cdot\sinh\gamma_{1m}x\cdot\cos k_{1m}y \tag{10}$$

where

$$k_{1m}=\frac{m\pi}{s},\qquad m:\text{integer}$$

$$\gamma_{1m}=\sqrt{k_{1m}^2-k_T^2},\qquad k_T^2=k_0^2-\beta^2.$$

Applying the TE constraint conditions on l_6 that $\partial\phi_{h2}/\partial n=0$, we also find the trial eigenfunction in region II ($t\leqslant x\leqslant a$) that

$$\phi_{h2}=\sum_{n=0}^{\infty}b_{hn}\cdot\cosh\gamma_{2n}(a-x)\cdot\cos k_{2n}y \tag{11}$$

where

$$k_{2n}=\frac{n\pi}{b},\qquad n:\text{integer}$$

$$\gamma_{2n}=\sqrt{k_{2n}^2-k_T^2}.$$

Similarly for TM modes, the trial eigenfunction ϕ_{ei} can be selected as

$$\phi_{e1}=\sum_{m=1}^{\infty}a_{em}\cdot\cosh\gamma_{1m}x\cdot\sin k_{1m}y \tag{12}$$

$$\phi_{e2}=\sum_{n=1}^{\infty}b_{en}\cdot\sinh\gamma_{2n}(a-x)\cdot\sin k_{2n}y. \tag{13}$$

And then we must consider the remaining constraints: the constraint given by (4b) on only l_5 and the constraint given by (4c) on l_3 for TE modes. Therefore, the unknown coefficients a_{hm} and b_{hn} should be decided to satisfy these constraint conditions. The unknown coefficients a_{em} and b_{en} should be decided to satisfy the remaining constraints for TM modes: the constraint given by (5b) on only l_5 and the constraint given by (5c) on l_3.

Substituting (10) and (11), or (12) and (13) into (4c) or (5c), and multiplying both members by $\cos k_{1m}y$ or $\cos k_{2n}y$ for TE modes, by $\sin k_{1m}y$ or $\sin k_{2n}y$ for TM modes, and then integrating from $y=0$ to s or b, the unknown coefficients are obtained by the orthogonal condition

$$a_{hm}=\frac{\epsilon_m}{s}\cdot\frac{\langle\xi\cdot\cos k_{1m}y\rangle_{l_3}}{\gamma_{1m}\cdot\cosh\gamma_{1m}t}$$

$$b_{hn}=-\frac{\epsilon_n}{b}\cdot\frac{\langle\xi\cdot\cos k_{2n}y\rangle_{l_3}}{\gamma_{2n}\cdot\sinh\gamma_{2n}h}$$

$$a_{em}=\frac{1}{s}\cdot\frac{\langle\eta\cdot\sin k_{1m}y\rangle_{l_3}}{\cosh\gamma_{1m}t}$$

$$b_{en}=\frac{1}{b}\cdot\frac{\langle\eta\cdot\sin k_{2n}y\rangle_{l_3}}{\sinh\gamma_{2n}h} \tag{14}$$

where

$$h = a - t$$
$$\epsilon_0 = 1, \quad \epsilon_m (m \geqslant 1) = \epsilon_n (n \geqslant 1) = 2.$$

Next, we should select the appropriate trial distribution function $\xi(y)$ which is proportional to the y component of the electric field on l_3. In the case of a ridged waveguide, as the edge of the ridge has a right angle, the y component of an electric field near the edge is approximately proportional to $\Delta y^{-(1/3)}$ [13], where Δy means the distance between an edge and an observational point. Therefore, by using an arbitrary constant C_q, $\xi(y)$ is given by

$$\xi(y) = \begin{cases} \sum_{q=0}^{\infty} C_q \cdot \cos k_q y \cdot (s^2 - y^2)^{-(1/3)}, & |y| \leqslant s \\ 0, & |y| > s \end{cases} \tag{15}$$

where

$$k_q = \frac{q\pi}{s}, \qquad q: \text{integer}.$$

For TM modes, the trial distribution function $\eta(y)$ and $\xi(y)$ which are proportional to the z and y components of the electric field on l_3 can exhibit the relations $\eta \propto \phi_{et}$ and $\xi \propto \partial\phi_{et}/\partial y$ by using (2b). And the following relation can be obtained:

$$\xi \propto \frac{d\eta}{dy}. \tag{16}$$

By using the partial integral

$$\langle \eta \cdot \sin k_{1m} y \rangle_{l_3} = \frac{1}{k_{1m}} \left\{ \int_0^s \frac{d\eta}{dy} \cdot \cos k_{1m} y \cdot dy - \eta(s) + \eta(0) \right\}. \tag{17}$$

By substituting (16) and the relation $\eta(s) = \eta(0) = 0$, the following relations can be obtained:

$$\langle \eta \cdot \sin k_{1m} y \rangle_{l_3} = \frac{K}{k_{1m}} \cdot \langle \xi \cdot \cos k_{1m} y \rangle_{l_3} \tag{18a}$$

$$\langle \eta \cdot \sin k_{2n} y \rangle_{l_3} = \frac{K}{k_{2n}} \cdot \langle \xi \cdot \cos k_{2n} y \rangle_{l_3} \tag{18b}$$

where K is an arbitrary constant.

When using (10), (11), and (14), and the constraint conditions given by (4b) and (4c), (7a) becomes

$$\langle \phi_{h1} \cdot \xi \rangle_{l_3} - \langle \phi_{h2} \cdot \xi \rangle_{l_3} = 0. \tag{19}$$

Similarly for TM modes, the following relation is obtained:

$$\left\langle \frac{\partial \phi_{e1}}{\partial x} \cdot \eta \right\rangle_{l_3} - \left\langle \frac{\partial \phi_{e2}}{\partial x} \cdot \eta \right\rangle_{l_3} = 0. \tag{20}$$

The Fourier transforms of the trial distribution function $\xi(y)$ in regions I and II are defined as $\tilde{\xi}_m$ and $\bar{\xi}_n$, respectively, where $\tilde{\xi}_m$ and $\bar{\xi}_n$ are given in Appendix III.

Substituting (10)–(14), (18), and (A16) into (19) and (20), stationary eigenvalue formulas can be obtained

for TE modes

$$\frac{1}{s} \sum_{m=0}^{\infty} \epsilon_m \cdot \frac{\tanh \gamma_{1m} t}{\gamma_{1m}} \cdot \tilde{\xi}_m^2 + \frac{1}{b} \sum_{n=0}^{\infty} \epsilon_n \cdot \frac{\coth \gamma_{2n} h}{\gamma_{2n}} \cdot \bar{\xi}_n^2 = 0 \tag{21a}$$

$$P_h = \text{left-hand side of (21a)} \tag{21b}$$

for TM modes

$$s \sum_{m=1}^{\infty} \frac{\gamma_{1m} \cdot \tanh \gamma_{1m} t}{m^2} \cdot \tilde{\xi}_m^2 + b \sum_{n=1}^{\infty} \frac{\gamma_{2n} \cdot \coth \gamma_{2n} h}{n^2} \bar{\xi}_n^2 = 0 \tag{22a}$$

$$P_e = \text{left-hand side of (22a)} \tag{22b}$$

where P_h and P_e are stationary for ξ, because they are derived from the left-hand side of (7a) and (9), which are stationary for ϕ_{hi} and ϕ_{ei}, respectively.

Considering only the comparative lower order modes in the y coordinate, we retain the first three terms (i.e., $q \leqslant 2$) in (A16) for $\tilde{\xi}_m$ and $\bar{\xi}_n$. Since P_h given by (21b) is stationary for ξ, for the TE modes, letting $C_0 = 1$, C_1 and C_2 are obtained from (23a) by using the Rayleigh–Ritz procedure [14]. Similarly, for the TM modes, letting $C_1 = 1$, C_0 and C_2 are obtained from (23b)

for TE modes

$$\partial P_h / \partial C_1 = 0, \quad \partial P_h / \partial C_2 = 0 \tag{23a}$$

for TM modes

$$\partial P_e / \partial C_0 = 0, \quad \partial P_e / \partial C_2 = 0. \tag{23b}$$

V. Numerical Results of Eigenvalue Problems

Montgomery defined two kinds of eigenmodes for the double-ridged waveguide [5], i.e., Hybrid modes and Trough modes. The Hybrid mode is considered to be a basic ridged waveguide mode and the Trough mode is a rectangular waveguide-type mode which exists in the trough region, region II. These definitions are also used in this present paper. TE and TM modes are further classified into TE Hybrid, TE Trough, TM Hybrid, and TM Trough modes.

The eigenvalues of the transverse propagation constant $k_T (= \sqrt{k_0^2 - \beta^2})$ can be obtained from (21), (22), and (23) by numerical calculation using the bisection method. In the actual computations of (21) and (22), the summations over m and n are terminated when $m = 20$ and $n = 30$ with enough accuracy where examining the convergence of the variation of the eigenvalue as a function of m and n. For example, by comparing the eigenvalues of this proposed analysis with those of [5] for the double-ridged waveguide shown in Table II, both eigenvalues exhibit a good agreement within an error margin less than 0.6 percent for $m = 20$ and $n = 30$, and less than 0.4 percent for $m = 50$

TABLE I
ODD-MODE EIGENVALUE K_T OF SINGLE-RIDGED WAVEGUIDE AND CORRESPONDENT EIGENMODE OF RECTANGULAR WAVEGUIDE (USING WRJ-120 WAVEGUIDE)

rectangular waveguide (2a×b) a=b=9 5(mm)		mode transition	ridged waveguide (2a×b,2t,s) a=b=9 5, t=0 15, s=1 7(mm)		
eigenvalue k_T(rad/mm)	mode name		mode name	eigenvalue k_T(rad/mm)	rectangular waveguide (b×h) eigenvalue k_T(rad/mm)
0 1653	TE_{10}	→	TE_{10} Hybrid	0 0930	
0 3697	TE_{11}	→	TE_{10} Trough	0 3332	0 3307
0 3697	TM_{11}	×	TE_{30} Hybrid	0 3881	
0 4960	TE_{30}	×	TM_{11} Trough	0 4665	0 4714
0 5962	TE_{31}	→	TE_{31} Hybrid	0 5265	
0 6817	TE_{12}	→	TE_{20} Trough	0 6654	0 6614
0 6817	TM_{12}	×	TE_{50} Hybrid	0 6913	
0 8267	TE_{50}	×	TM_{12} Trough	0 7358	0 7490
0 8267	TE_{32}	→	TE_{21} Trough	0 7456	0 7418
0 8267	TM_{22}	×	TE_{51} Hybrid	0 8298	
0 8904	TE_{51}	×	TM_{22} Trough	0 9427	0 9429

and $n = 200$. The first eleven eigenvalues are obtained for the single-ridged waveguide using a WRJ-120 waveguide ($2a = 19.0$ mm, $b = 9.5$ mm) and $2t = 0.3$ mm, $s = 1.7$ mm, which is the typical example of a PCMW in the 12-GHz-band low-noise down converter [9], [10] for satellite broadcasting. These results are shown in Table I. In this table, it is evident that eigenvalues of Trough modes are almost equal to those of a rectangular waveguide whose dimensions are $b \times h$. All eigenvalues of a ridged waveguide originate from those of a rectangular waveguide with dimensions $2a \times b$ as shown in Table I. When the value of s increases to 9.5 mm, that is, the limit at which the ridge vanishes, eigenvalues of a ridged waveguide are astringent to those of a rectangular waveguide. These correspondences are shown in Fig. 3.

For the first four modes shown in Table I, the relation between the normalized eigenvalue, $k_T a$ and s/b in the case of $a = b$ with several values of the parameter t/a is shown in Fig. 3. In the Hybrid mode, the energy is concentrated in the gap of the ridge. Therefore, by making the value of s/b larger, the value of $k_T a$ becomes larger because of the smoothing in the curvature of the magnetic flux near the gap. In the Trough mode for a small gap, the main part of its energy does not exist under the gap. By varying the values of s/b and t/a, the value of $k_T a$ is constant with respect to s/b when $s/b \leqslant 0.4$, and this confirms that $k_T a$ is related to the $b \times h$ dimensions of the rectangular waveguide only.

As the value of s/b increases to one, the limit value of $k_T a$ is astringent to the eigenvalue of the rectangular waveguide whose dimensions are $2a \times b$, as described above. These transitions are explained later in Fig. 4.

For the TE_{10} Hybrid mode, by using Getsinger's approximated field distributions [4], the eigenvalues can be calculated by the variational method. These results plotted by dots in Fig. 3 are in good agreement with the theoretical values described in this paper.

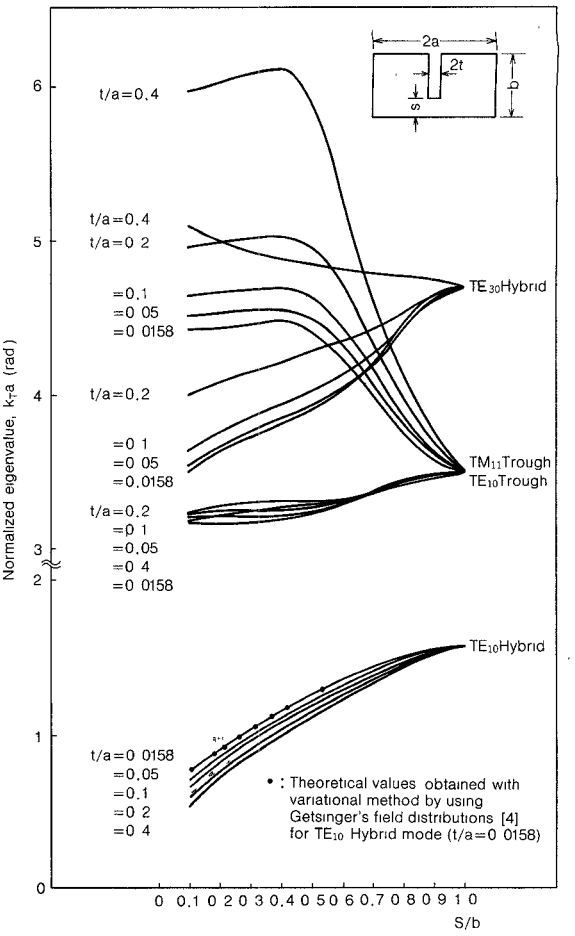

Fig. 3. Relation between normalized eigenvalue $k_T a$ versus s/b and t/a (with $a = b$).

TABLE II
ODD-MODE EIGENVALUE K_T OF DOUBLE-RIDGED WAVEGUIDE——. COMPARISON BETWEEN THIS PROPOSED ANALYSIS AND THE ONE FOUND IN [5].

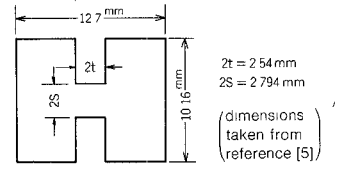

mode name	k_T(rad/mm) this present analysis	k_T(rad/mm) reference [5]
TE_{10} Hybrid	0 1438	0 1437
TE_{10} Trough	0 3155	0 3166
TE_{20} Trough	0 6215	0 6190
TE_{30} Hybrid	0 6707	0 6712
TE_{11} Trough	0 6971	0 6973

The eigenvalues of the double-ridged waveguide whose dimensions are taken from [5] are obtained by using this proposed analysis. The results are compared in Table II. Both eigenvalues exhibit a good agreement within an error margin of 0.07–0.4 percent, and this agreement ensures the propriety of this proposed analysis.

VI. Normal Mode Formulation of Transverse Fields

The normal modes of the TE and TM transverse fields are expressed by

for TE modes

$$\boldsymbol{e}_{ht} = \boldsymbol{i}_x e_{hx} + \boldsymbol{i}_y e_{hy}$$
$$\boldsymbol{h}_{ht} = \boldsymbol{i}_x h_{hx} + \boldsymbol{i}_y h_{hy} \tag{24a}$$

for TM modes

$$\boldsymbol{e}_{et} = \boldsymbol{i}_x e_{ex} + \boldsymbol{i}_y e_{ey}$$
$$\boldsymbol{h}_{et} = \boldsymbol{i}_x h_{ex} + \boldsymbol{i}_y h_{ey} \tag{24b}$$

where the transmitting power is normalized as a unit value, and $\boldsymbol{i}_x$ and $\boldsymbol{i}_y$ are the unit vectors in the x or y coordinates, respectively. From (2), (10)–(14), (18), and (A16), every component of the normal modes given in (24) can be obtained as

for TE modes

$$e_{hx1} = h_{hy1} = A_l \frac{1}{s} \sum_{m=1}^{\infty} \frac{k_{1m} \cdot \sinh \gamma_{1m} x}{\gamma_{1m} \cdot \cosh \gamma_{1m} t} \cdot \bar{\xi}_m \cdot \sin k_{1m} y$$

$$e_{hy1} = -h_{hx1} = A_l \frac{1}{2s} \sum_{m=0}^{\infty} \epsilon_m \cdot \frac{\cosh \gamma_{1m} x}{\cosh \gamma_{1m} t} \cdot \bar{\xi}_m \cdot \cos k_{1m} y$$

$$e_{hx2} = h_{hy2} = -A_l \frac{1}{b} \sum_{n=1}^{\infty} \frac{k_{2n} \cdot \cosh \gamma_{2n}(a-x)}{\gamma_{2n} \cdot \sinh \gamma_{2n} h} \cdot \bar{\xi}_n \cdot \sin k_{2n} y$$

$$e_{hy2} = -h_{hx2} = A_l \frac{1}{2b} \sum_{n=0}^{\infty} \epsilon_n \cdot \frac{\sinh \gamma_{2n}(a-x)}{\sinh \gamma_{2n} h} \cdot \bar{\xi}_n \cdot \cos k_{2n} y \tag{25a}$$

for TM modes

$$e_{ex1} = h_{ey1} = A_l \frac{1}{s} \sum_{m=1}^{\infty} \frac{\gamma_{1m} \cdot \sinh \gamma_{1m} x}{k_{1m} \cdot \cosh \gamma_{1m} t} \cdot \bar{\xi}_m \cdot \sin k_{1m} y$$

$$e_{ey1} = -h_{ex1} = A_l \frac{1}{s} \sum_{m=1}^{\infty} \frac{\cosh \gamma_{1m} x}{\cosh \gamma_{1m} t} \cdot \bar{\xi}_m \cdot \cos k_{1m} y$$

$$e_{ex2} = h_{ey2} = -A_l \frac{1}{b} \sum_{n=1}^{\infty} \frac{\gamma_{2n} \cdot \cosh \gamma_{2n}(a-x)}{k_{2n} \cdot \sinh \gamma_{2n} h} \cdot \bar{\xi}_n \cdot \sin k_{2n} y$$

$$e_{ey2} = -h_{ex2} = A_l \frac{1}{b} \sum_{n=1}^{\infty} \frac{\sinh \gamma_{2n}(a-x)}{\sinh \gamma_{2n} h} \cdot \bar{\xi}_n \cdot \cos k_{2n} y \tag{25b}$$

where the suffixes 1 and 2 mean regions I and II, respectively, and A_l means the normalizing coefficient of the lth mode.

In addition, the normal modes given by (25) are satisfied with the orthogonal condition given by (26), which is confirmed by numerical calculation

$$\int\int_{S_r} \boldsymbol{e}_{tl}^* \times \boldsymbol{h}_{tl'} \cdot \boldsymbol{i}_z \, ds = \begin{cases} 1, & l = l' \\ 0, & l \neq l' \end{cases} \tag{26}$$

where $\boldsymbol{e}_{tl}$ and $\boldsymbol{h}_{tl'}$ express the transverse electric field of the lth mode and the transverse magnetic field of the l'th mode, respectively, S_r means a cross-sectional area of a ridged waveguide, and A^* means a complex conjugate of A.

From (25), the transverse electric-field profiles of the first four eigenmodes are obtained as shown in Fig. 4. The arrow indicates the direction of the field vector and its length is proportional to the logarithm of the field strength at every point. In Fig. 4(d), the arrows in the second column from the left do not seem to be smooth. This is caused from the numerical error. Fig. 4 also illustrates how mode transition occurs from a waveguide eigenmode to a ridged waveguide eigenmode corresponding to the value of s/b.

VII. Guide Wavelength and Characteristic Impedance of Dominant Mode

A. Guide Wavelength

The guide waveglength λ_g can generally be obtained from the eigenvalue k_T as

$$\lambda_g = \frac{\lambda_0}{\sqrt{1-(\lambda_0/\lambda_c)^2}} \tag{27}$$

where

$\lambda_c = 2\pi/k_T$ cutoff wavelength
λ_0 free-space wavelength.

For the TE_{10} Hybrid mode, the frequency dependent λ_g is calculated from the value of k_T in Table I and (27), and the result is shown in Fig. 5, by using the WRJ-120 waveguide and $2t = 0.3$ mm, $s = 1.7$ mm. In Fig. 5, the experimental values of λ_g obtained from the resonant frequency of the slot resonator are shown together. These experimental values have been corrected by the short-end effect correction length Δl of the short-ended ridged waveguide [15]. The theoretical values are in good agreement with these experimental ones. From Fig. 5, it is evident that the value of λ_g has a frequency dispersion.

B. Characteristic Impedance

The characteristic impedance Z_c of the TE_{10} Hybrid mode can be expressed by using the definition of [7]

$$Z_c = V_y^2/(2P)$$
$$V_y = \int_0^s E_y(0, y) \cdot dy$$
$$P = (1/2) \cdot \mathrm{Re} \int_0^b \int_0^a \left(E_y H_x^* - E_x H_y^* \right) \cdot dx \cdot dy \tag{28}$$

where V_y means the gap voltage across the ridged waveguide at $x = 0$, P the average transmitting power, and Re means the real part. Substituting (2), (10)–(14), (18), and

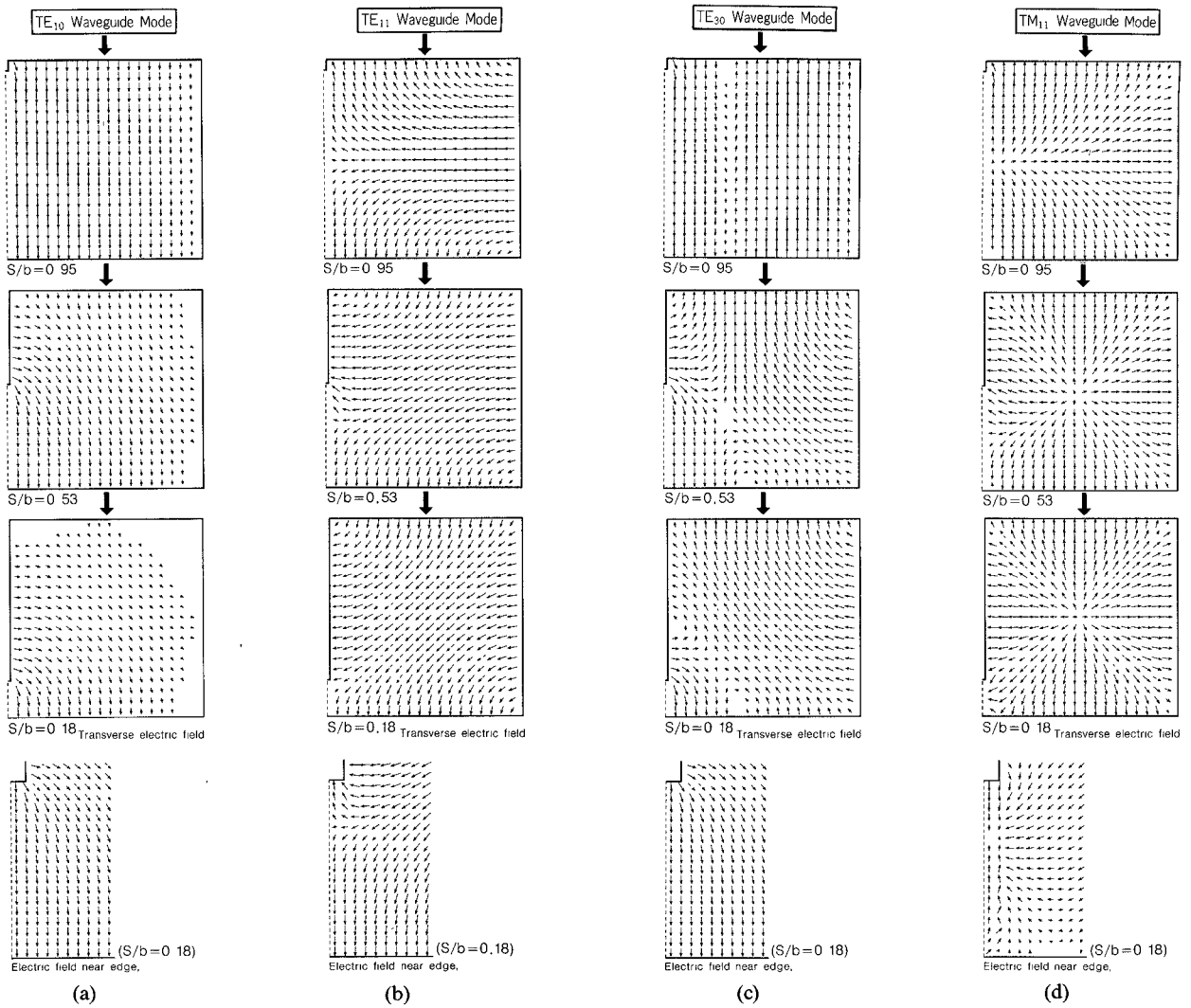

Fig. 4. Transverse electric-field profile of single-ridged waveguide eigenmode and its mode transition from rectangular waveguide eigenmode (with $a = b, t/a = 0.016$). (a) TE_{10} Hybrid mode, (b) TE_{10} Trough mode, (c) TE_{30} Hybrid mode, and (d) TM_{11} Trough mode.

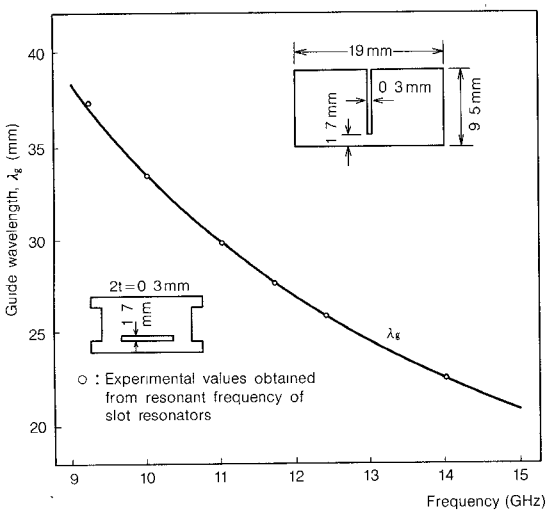

Fig. 5. Frequency dependence of guide wavelength λg of TE_{10} Hybrid mode (using WRJ-120 waveguide and $2t = 0.3$ mm, $s = 1.7$ mm).

(A16) into (28), Z_c is obtained

$$Z_c = \frac{Z_{c\infty}}{\sqrt{1-(k_T/k_0)^2}}$$

$$Z_{c\infty} = \frac{60\pi \cdot \tilde{\xi}_0^2}{(P_1+P_2)\cdot\cos^2\gamma_{10}t}$$

$$P_1 = \frac{1}{2s}\sum_{m=0}^{\infty}\frac{\epsilon_m\cdot\tilde{\xi}_m^2}{\cosh^2\gamma_{1m}t} \cdot\left[\frac{\sinh 2\gamma_{1m}t}{2\gamma_{1m}}\cdot\left\{1+\left(\frac{k_{1m}}{\gamma_{1m}}\right)^2\right\}+t\cdot\left\{1-\left(\frac{k_{1m}}{\gamma_{1m}}\right)^2\right\}\right]$$

$$P_2 = \frac{1}{2b}\sum_{n=0}^{\infty}\frac{\epsilon_n\cdot\bar{\xi}_n^2}{\sinh^2\gamma_{2n}h} \cdot\left[\frac{\sinh 2\gamma_{2n}h}{2\gamma_{2n}}\cdot\left\{1+\left(\frac{k_{2n}}{\gamma_{2n}}\right)^2\right\}-h\cdot\left\{1-\left(\frac{k_{2n}}{\gamma_{2n}}\right)^2\right\}\right] \quad (29)$$

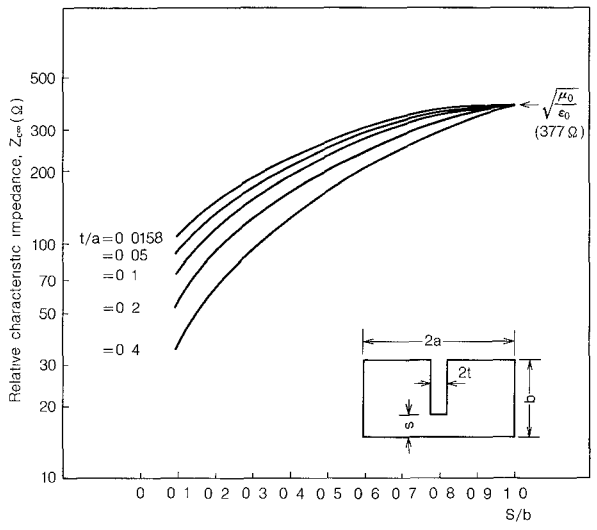

Fig. 6. Relation between relative characteristic impedance $Z_{c\infty}$ versus s/b and t/a (with $a=b$).

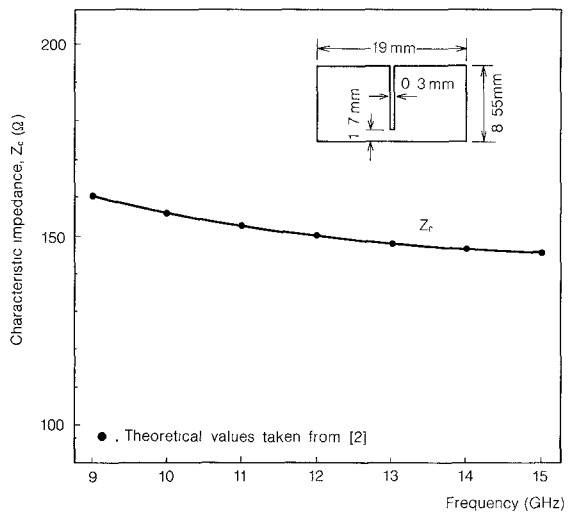

Fig. 7. Frequency dependence of characteristic impedance Z_c of TE_{10} Hybrid mode (with $2a=19.0$ mm, $b=8.55$ mm, $2t=0.3$ mm, and $s=1.7$ mm)

where the relative characteristic impedance $Z_{c\infty}$ is the corresponding value of Z_c at the infinitely high frequency.

From (29), the relation between $Z_{c\infty}$ and s/b in the case of $a=b$ is calculated for several values of t/a, and is shown in Fig. 6. In Fig. 6, as the value of s/b increases to one, the value of $Z_{c\infty}$ becomes astringent to $\sqrt{\mu_0/\epsilon_0}$ ($=377\ \Omega$), the intrinsic impedance of free space. In the case of a waveguide where $2a=19.0$ mm, $b=8.55$ mm, $2t=0.3$ mm, and $s=1.7$ mm, the frequency dependence of Z_c is obtained as shown in Fig. 7. The theoretical values of [2], where $b=0.9a$, are plotted by dots in Fig. 7. Both theoretical values have a good agreement.

VIII. Conclusion

For the analysis of a ridged waveguide, a simplified variational method has been proposed. By using this theoretical method, the eigenvalue formula, the normal mode expression, the electric-field profile, the guide wavelength, and the characteristic impedance of the dominant mode can be obtained, and the fundamental design charts of a ridged waveguide have been given. The correspondence between the eigenmode of a ridged waveguide and the original one of a rectangular waveguide were obtained. And the normal mode expressions given in this paper will be useful for the determination of several kinds of equivalent circuits for discontinuities in a ridged waveguide.

Appendix I
Proof of Stationary Character of (4) and (5)

Equations (4a) and (5a) can be summarized in the following stationary formula:

$$k_T^2 = -\frac{\sum_{i=1}^{2}\langle\phi_{pi}\cdot\nabla_t^2\phi_{pi}\rangle_{S_i} \pm \sum_{i=1}^{2}\langle\phi_{pi}\cdot\frac{\partial\phi_{pi}}{\partial n}\rangle_{C_i}}{\sum_{i=1}^{2}\langle\phi_{pi}^2\rangle_{S_i}}. \quad \text{(A1)}$$

In this Appendix, it should be proved that if ϕ_{pi} $(i=1,2)$ minimize (A1) with the constraints given by (4b) and (4c), or (5b) and (5c), then they are the correct solutions of (1) with proper boundary conditions.

When taking the positive sign in (A1), the following relation can be obtained by letting ϕ_{pi} vary a small amount $\delta\phi_{pi}$:

$$\begin{aligned}2k_T\cdot\sum_{i=1}^{2}\langle\phi_{pi}^2\rangle_{S_i}\cdot\delta k_T &= -2k_T^2\cdot\sum_{i=1}^{2}\langle\phi_{pi}\cdot\delta\phi_{pi}\rangle_{S_i}\\ &\quad-\sum_{i=1}^{2}\langle\delta\phi_{pi}\cdot\nabla_t^2\phi_{pi}\rangle_{S_i}-\sum_{i=1}^{2}\langle\phi_{pi}\cdot\nabla_t^2\delta\phi_{pi}\rangle_{S_i}\\ &\quad-\sum_{i=1}^{2}\langle\delta\phi_{pi}\cdot\frac{\partial\phi_{pi}}{\partial n}\rangle_{C_i}-\sum_{i=1}^{2}\langle\phi_{pi}\cdot\frac{\partial\delta\phi_{pi}}{\partial n}\rangle_{C_i}.\end{aligned} \quad \text{(A2)}$$

By using the Green's first identity in the fourth and fifth terms of the right-hand side of (A2), (A2) can be transformed into

$$\begin{aligned}k_T\cdot\sum_{i=1}^{2}\langle\phi_{pi}^2\rangle_{S_i}\cdot\delta k_T &= -\sum_{i=1}^{2}\langle\delta\phi_{pi}\cdot\left(\nabla_t^2\phi_{pi}+k_T^2\phi_{pi}\right)\rangle_{S_i}\\ &\quad-\sum_{i=1}^{2}\langle\phi_{pi}\cdot\frac{\partial\delta\phi_{pi}}{\partial n}\rangle_{C_i}.\end{aligned} \quad \text{(A3)}$$

For the TE modes, if the trial eigenfunction is selected to satisfy the constraints on the conductor surfaces l_2, l_4, l_5, and l_6 as shown in (4b), the second term of the right-hand side of (A3) can be transformed into

$$\sum_{i=1}^{2}\langle\phi_{hi}\cdot\frac{\partial\delta\phi_{hi}}{\partial n}\rangle_{C_i}=\langle\phi_{h1}\cdot\frac{\partial\delta\phi_{h1}}{\partial x}\rangle_{l_1+l_3}-\langle\phi_{h_2}\cdot\frac{\partial\delta\phi_{h2}}{\partial x}\rangle_{l_3} \quad \text{(A4)}$$

where $\langle A\rangle_{l_1+l_3}$ signifies $\langle A\rangle_{l_1}+\langle A\rangle_{l_3}$. Then, if the trial eigenfunction is also selected to satisfy the continuity con-

TABLE III
STATIONARY CHARACTER OF (A1)

stationary formula	stationary condition	mode	constraint conditions for trial eigenfunction	
$k_T^2 = -\dfrac{\sum_{i=1}^{2}\langle\phi_{pi}\cdot\nabla_t^2\phi_{pi}\rangle_{S_i}+\sum_{i=1}^{2}\langle\phi_{pi}\cdot\frac{\partial\phi_{pi}}{\partial n}\rangle_{C_i}}{\sum_{i=1}^{2}\langle\phi_{pi}^2\rangle_{S_i}}$	$\sum_{i=1}^{2}\langle\phi_{pi}\cdot\frac{\partial\delta\phi_{pi}}{\partial n}\rangle_{C_i}=0$	TE	$\frac{\partial\phi_{h1}}{\partial n}=0$ on ℓ_2,ℓ_4,ℓ_5 and ℓ_6 $\frac{\partial\phi_{h1}}{\partial n}=\frac{\partial\phi_{h2}}{\partial n}$ on ℓ_3	$\Rightarrow$ eq. (4)
		TM	$\frac{\partial\phi_{e1}}{\partial n}=0$ on ℓ_1 $\frac{\partial\phi_{e1}}{\partial n}=\frac{\partial\phi_{e2}}{\partial n}$ on ℓ_3	
$k_T^2 = -\dfrac{\sum_{i=1}^{2}\langle\phi_{pi}\cdot\nabla_t^2\phi_{pi}\rangle_{S_i}-\sum_{i=1}^{2}\langle\phi_{pi}\cdot\frac{\partial\phi_{pi}}{\partial n}\rangle_{C_i}}{\sum_{i=1}^{2}\langle\phi_{pi}^2\rangle_{S_i}}$	$\sum_{i=1}^{2}\langle\delta\phi_{pi}\cdot\frac{\partial\phi_{pi}}{\partial n}\rangle_{C_i}=0$	TE	$\phi_{e1}=0$ on ℓ_1 $\phi_{e1}=\phi_{e2}$ on ℓ_3	
		TM	$\phi_{ei}=0$ on ℓ_2,ℓ_4,ℓ_5 and ℓ_6 $\phi_{e1}=\phi_{e2}$ on ℓ_3	$\Rightarrow$ eq. (5)

dition of the tangential component of the electric field as shown in (4c), (A4) becomes

$$\sum_{i=1}^{2}\langle\phi_{hi}\cdot\frac{\partial\delta\phi_{hi}}{\partial n}\rangle_{C_i}=\langle\phi_{h1}\cdot\frac{\partial\delta\phi_{h1}}{\partial x}\rangle_{l_1}+\langle\xi\cdot(\phi_{h1}-\phi_{h2})\rangle_{l_3}. \tag{A5}$$

As the right-hand side of (A5) vanishes with the boundary condition on the magnetic wall l_1 and the continuity condition on l_3, the following relation can be obtained:

$$\sum_{i=1}^{2}\langle\phi_{hi}\cdot\frac{\partial\delta\phi_{hi}}{\partial n}\rangle_{C_i}=0. \tag{A6}$$

Therefore, (A3) becomes

$$k_T\cdot\sum_{i=1}^{2}\langle\phi_{hi}^2\rangle_{S_i}\cdot\delta k_T=-\sum_{i=1}^{2}\langle\delta\phi_{hi}\cdot(\nabla_t^2\phi_{hi}+k_T^2\phi_{hi})\rangle_{S_i}. \tag{A7}$$

When $\delta k_T=0$, ϕ_{hi} are the correct solutions of (1) with the above boundary conditions on l_1 and l_3.

Similarly for the TM modes, if the trial eigenfunction is selected to satisfy the constraint condition on l_1 and l_3 in Table III, the second term of the right-hand side of (A3) vanishes as shown in (A8) by using the boundary condition on the conductor surfaces l_2, l_4, l_5, and l_6

$$\sum_{i=1}^{2}\langle\phi_{ei}\cdot\frac{\partial\delta\phi_{ei}}{\partial n}\rangle_{C_i}=0. \tag{A8}$$

Therefore, (A3) becomes

$$k_T\cdot\sum_{i=1}^{2}\langle\phi_{ei}^2\rangle_{S_i}\cdot\delta k_T=-\sum_{i=1}^{2}\langle\delta\phi_{ei}\cdot(\nabla_t^2\phi_{ei}+k_T^2\phi_{ei})\rangle_{S_i}. \tag{A9}$$

When $\delta k_T=0$, δ_{ei} are also the correct solutions of (1) with the above boundary conditions on l_2, l_4, l_5, and l_6.

In the case of taking the negative sign in (A1), the following relation can be obtained:

$$k_T\cdot\sum_{i=1}^{2}\langle\phi_{pi}^2\rangle_{S_i}\cdot\delta k_T=-\sum_{i=1}^{2}\langle\delta\phi_{pi}\cdot(\nabla_t^2\phi_{pi}+k_T^2\phi_{pi})\rangle_{S_i}+\sum_{i=1}^{2}\langle\delta\phi_{pi}\cdot\frac{\partial\phi_{pi}}{\partial n}\rangle_{C_i}. \tag{A10}$$

For TM modes, the relation of (A11) can be obtained

$$\sum_{i=1}^{2}\langle\delta\phi_{ei}\cdot\frac{\partial\phi_{ei}}{\partial n}\rangle_{C_i}=0 \tag{A11}$$

under the constraint conditions given by (5b) and (5c) and the proper boundary conditions. For TE modes, the relation of (A12) can be obtained

$$\sum_{i=1}^{2}\langle\delta\phi_{hi}\cdot\frac{\partial\phi_{hi}}{\partial n}\rangle_{C_i}=0 \tag{A12}$$

under the constraint conditions on l_1 and l_3 for the trial eigenfunctions shown in Table III, and the proper boundary conditions.

When $\delta k_T=0$ in (A10), ϕ_{hi} and ϕ_{ei} are the correct solutions of (1) by using the relations of (A11) and (A12), respectively. The proof of the stationary character of (A1) is completed for both TE and TM modes. These results are summarized in Table III.

In order to use the known distribution functions $\xi(y)$ and $\eta(y)$ which are proportional to the tangential components of the electric field on l_3 as the trial distribution functions, (A1) with the positive sign is selected as the variational expression for k_T^2 in the case of the TE modes as shown in (4) and Table III, and (A1) with the negative sign is selected as the variational expression for k_T^2 in the case of the TM modes as shown in (5) and Table III.

APPENDIX II
DERIVATION OF (8)

In (7a), let ϕ_{hi} vary a small amount, a parameter p_1 times an error function e_1 plus a parameter p_2 times an error function e_2 about its correct function ϕ_{hi}^c shown as

$$\phi_{hi} = \phi_{hi}^c + p_1(k_T^2)e_1 + p_2 e_2 \tag{A13}$$

where $p_1\{ \equiv p_1(k_T^2)\}$ is a function of k_T^2, and $p_1(k_T^2)e_1$ is corresponding to the error resulted from the difference between k_T and its correct value k_T^C, and $p_1(k_T^{C^2}) = 0$. On the contrary, $p_2 e_2$ is independent on k_T, and is corresponding to the error caused by the finite number terminations (m and n) on the summations appeared in (10) and (11).

From (7b) and (A13), $F\{ \equiv F(k_T^2, p_2)\}$ can be considered as a function of k_T^2 and p_2, and then (7a) becomes

$$F(k_T^2, p_2) = 0. \tag{A14}$$

Equation (A14) constrains F to vanish; hence, as k_T^2 and p_2 are varied [16], we have

$$\left.\frac{\partial F}{\partial k_T^2}\right|_{\substack{k_T^2 = k_T^{C^2} \\ p_2 = 0}} \cdot \delta k_T^2 + \left.\frac{\partial F}{\partial p_2}\right|_{\substack{k_T^2 = k_T^{C^2} \\ P_2 = 0}} \cdot \delta p_2 = 0 \tag{A15}$$

where $k_T^{c^2}$ signifies the correct value of k_T^2.

The second term of this equation vanishes because F is stationary about $p_1 = 0$ (i.e., $k_T^2 = k_T^{c^2}$) and $p_2 = 0$ for ϕ_{hi} as described in Section III-B. The coefficient of the first term is not, in general, zero; thus, the relation shown in (8) is derived.

APPENDIX III
FOURIER TRANSFORMS OF $\xi(y)$

The Fourier transform of $\xi(y)$ for k_{1m} and k_{2n} in regions I and II are expressed by $\tilde{\xi}_m$ and $\bar{\xi}_n$, respectively, and given by

$$\tilde{\xi}_m = \langle \xi(y) \cdot \cos k_{1m} y \rangle_{l_3} = \sum_{q=0}^{\infty} C_q \cdot \tilde{\xi}_{qm}$$

$$\tilde{\xi}_{qm} = \{(m+q)\pi\}^{-(1/6)} \cdot J_{1/6}\{(m+q)\pi\} + \{|m-q|\pi\}^{-(1/6)} \cdot J_{1/6}\{|m-q|\pi\} \tag{A16a}$$

$$\bar{\xi}_n = \langle \xi(y) \cdot \cos k_{2n} y \rangle_{l_3} = \langle \xi(y) \cdot \cos k_{2n} y \rangle_{l_3 + l_5} = \sum_{q=0}^{\infty} C_q \cdot \bar{\xi}_{qn}$$

$$\bar{\xi}_{qn} = \left\{\left(\frac{s}{b}n + q\right)\pi\right\}^{-(1/6)} \cdot J_{1/6}\left\{\left(\frac{s}{b}n + q\right)\pi\right\} + \left\{\left|\frac{s}{b}n - q\right|\pi\right\}^{-(1/6)} \cdot J_{1/6}\left\{\left|\frac{s}{b}n - q\right|\pi\right\} \tag{A16b}$$

where $J_{1/6}$ is the Bessel function of the first kind.

By substituting (A16a) and (A16b) into (21), (22), and (23), eigenvalues can be obtained.

ACKNOWLEDGMENT

The author wishes to thank Dr. Y. Konishi, the Senior Executive Vice President at Uniden Corporation, and K. Nio, the Deputy Director, and Dr. K. Uenakada, the Manager of the Radio Engineering Research Division, at the NHK Technical Research Laboratories for their guidances and many helpful discussions. He also wishes to thank Dr. K. Oyamada and H. Matsumura of the same laboratories for their helpful discussions.

REFERENCES

[1] S. B. Cohn, "Properties of ridge waveguide," *Proc. IRE*, vol. 35, pp. 783–788, Aug. 1947.
[2] S. Hopfer, "The design of ridged waveguides," *IRE Trans. Microwave Theory Tech.*, vol. MTT-3, pp. 20–29, Oct. 1955.
[3] J. R. Pyle, "The cutoff wavelength of the TE_{10} mode in ridged rectangular waveguide of any aspect ratio," *IEEE Trans. Microwave Theory Tech.*, vol. MTT-14, pp. 175–183, Apr. 1966.
[4] W. J. Getsinger, "Ridged waveguide field description and application to directional couplers," *IRE Trans. Microwave Theory Tech.*, vol. MTT-10, pp. 41–50, Jan. 1962.
[5] J. P. Montgomery, "On the complete eigenvalue solution of ridged waveguide," *IEEE Trans. Microwave Theory Tech.*, vol. MTT-19, pp. 547–555, June 1971.
[6] W. J. R. Hoefer and M. N. Burton, "Closed-form expressions for the parameters of finned and ridged waveguides," *IEEE Trans. Microwave Theory Tech.*, vol. MTT-30, pp. 2190–2194, Dec. 1982.
[7] L. P. Schmidt and T. Itoh, "Spectral domain analysis of dominant and higher order modes in fin-lines," *IEEE Trans. Microwave Theory Tech.*, vol. MTT-28, pp. 981–985, Sept. 1980.
[8] Y. Konishi, K. Uenakada, N. Yazawa, N. Hoshino, and T. Takahashi, "Simplified 12-GHz low-noise converter with mounted planar circuit in waveguide," *IEEE Trans. Microwave Theory Tech.*, vol. MTT-22, pp. 451–454, Apr. 1974.
[9] Y. Konishi, "12-GHz band FM receiver for satellite broadcasting," *IEEE Trans. Microwave Theory Tech.*, vol. MTT-26, pp. 720–725, Oct. 1978.
[10] Y. Utsumi, "Analysis of image recovery down converter made by planar circuit mounted in a waveguide," *IEEE Trans. Microwave Theory Tech.*, vol. MTT-30, pp. 858–868, June 1982.
[11] Y. Utsumi, "Variational analysis of ridged waveguide modes," Paper of Technical Group on Microwaves, MW83-63(1983-10), IECE Japan, pp. 23–30, Oct. 1983.
[12] R. F. Harrington, *Time-Harmonic Electromagnetic Fields*. New York: McGraw-Hill, 1961, ch. 3, pp. 129–130.
[13] R. E. Collin, *Field Theory of Guided Waves*. New York: McGraw-Hill, 1960, ch. 1, pp. 18–20.
[14] R. F. Harrington, *Time-Harmonic Electromagnetic Fields*. New York: McGraw-Hill, 1961, ch. 7, pp. 338–340.
[15] Y. Konishi and H. Matsumura, "Short end effect of ridge guide with planar circuit mounted in a waveguide," *IEEE Trans. Microwave Theory Tech.*, vol. MTT-27, pp. 168–170, Feb. 1979.
[16] R. F. Harrington, *Time-Harmonic Electromagnetic Fields*. New York: McGraw-Hill, 1961, ch. 7, pp. 340–345.

Yozo Utsumi (M'81) was born in Osaka, Japan, on August 3, 1943. He received the B. Eng., M. Eng., and the Dr. Eng. degrees from Osaka University (Osaka Daigaku), Osaka, Japan, in 1966, 1968 and 1984, respectively.

He joined Nippon Hoso Kyokai (Japan Broadcasting Corporation), Tokyo, in 1968. Since 1971, he has worked at their Technical Research Laboratories, where he has been engaged in research and development of VHF, UHF, and microwave circuits, and has been involved in the analysis and design of the low-noise receiver for satellite broadcasting. He had been the secretary and treasurer of IEEE MTT-S Tokyo Chapter in 1981 and 1982.

Dr. Utsumi is a member of IECEJ (Institute of Electrical Communication Engineering of Japan) and ITEJ (Institute of Television Engineering of Japan).